High-pressure Raman spectroscopy in the layered materials $2H$-MoS_2, $2H$-$MoSe_2$, and $2H$-$MoTe_2$

S. Sugai and T. Ueda
Department of Physics, Osaka University, Toyonaka, 560 Japan
(Received 8 January 1982)

Lattice vibrations were investigated by Raman spectroscopy in the layered materials $2H$-MoS_2 up to 180 kbar, $2H$-$MoSe_2$ up to 180 kbar, and $2H$-$MoTe_2$ up to 80 kbar. One A_{1g} and two E_{2g} modes were observed. The energies of the rigid-layer modes rapidly increase with pressure, but the increase becomes slow above 50 kbar. The interlayer and intralayer shear force constants are obtained as a function of pressure with the use of the linear-chain model.

INTRODUCTION

Transition-metal dichalcogenides have a typical layered crystal structure.[1] The two-dimensional lattice vibration is an interesting subject in conjunction with two-dimensional electronic-band structure and the effect of intercalation. The transition-metal IV dichalcogenides (TiX_2,ZrX_2,HfX_2), and the transition-metal VI dichalcogenides (MoX_2,WX_2) are all semiconductors with the exception of semimetallic $TiSe_2$.[2] The transition-metal V dichalcogenides (VX_2,NbX_2,TaX_2) are metallic and show the charge-density-wave phase transition due to the unique properties of the two-dimensional electronic-band structure.[3] These compounds are polymorphic. The basic structures are $1T$ and $2H$ structures. The molybdenum dichalcogenides crystallize in the $2H$ structure. In this structure the metal atom is surrounded by a trigonal prism of six chalcogen atoms. For molybdenum ditelluride there exists another structure, called the β structure, besides the normal α structure. In the β $2H$ structure, the metal atoms are located at deformed positions from the flat plane perpendicular to the c axis[1] and shows a phase transition at low temperatures.[4,5] The interlayer distances of these materials are large and the interlayer binding force comes from van der Waals force. The binding force between the interlayer chalcogen atoms are 2% or 3% of that between the intralayer metal and chalcogen atoms. The interlayer distance can be easily changed by external force applied to the crystal. We applied hydrostatic pressure to the crystal and observed the change of the inter- and intralayer forces through the lattice vibration.

The space group of $2H$-MoX_2 is D_{6h}^4 and one unit cell contains two molecules. The long-wavelength optical phonons are[6] $A_{1g}+A_{2u}+B_{1u}+2B_{2g}+E_{1g}+E_{1u}+2E_{2g}+E_{2u}$. The A_{2u} and E_{1u} modes are infrared active and the A_{1g}, E_{1g}, and E_{2g} modes are Raman active. In these crystals one unit cell contains two layers, and therefore the rigid-layer mode locates at the Γ point. The rigid-layer mode is the characteristic low-frequency mode reflecting the weak van der Waals binding force.[7] One of the B_{2g} and one of the E_{2g} modes correspond to this mode. The Raman active normal modes are shown in Fig. 1.

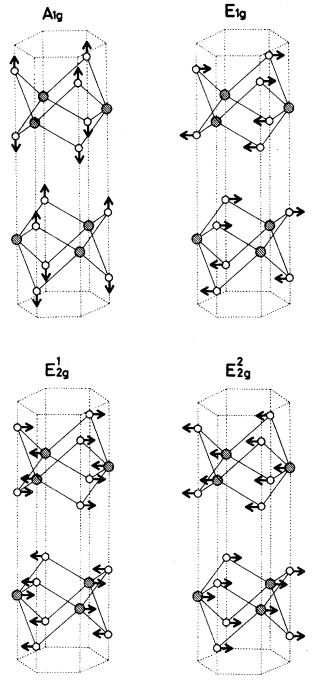

FIG. 1. Raman-active normal modes in $2H$-MoX_2. The large shaded circles represent molybdenum atoms and the small circles chalcogen atoms. The E_{2g}^2 mode is the rigid-layer mode.

At atmospheric pressure the lattice vibration has been observed by Raman scattering[6,8–15] and infrared spectroscopy.[8,16,17] Neutron-diffraction measurement[18] has been done in $2H$-MoS_2. High-pressure Raman scattering up to 50 kbar has been done in $2H$-MoS_2,[19] and the energy shift of the A_{1g} and E_{2g} modes, except the rigid-layer mode, have been observed. The electric resistivity, x-ray diffraction, and absorption spectra have been measured under high pressure in $2H$-MoS_2.[20–23] In this experiment, we measured the change of the energies of the A_{1g} and E_{2g} modes, including the rigid-layer mode up to 180 kbar in $2H$-MoS_2 and $2H$-$MoSe_2$ and up to 80 kbar in α-$2H$-$MoTe_2$, and we observed the change of interlayer van der Waals force and the intralayer binding force.

EXPERIMENTAL DETAILS AND RESULTS

Natural crystals were used for $2H$-MoS_2. The crystals of $2H$-$MoSe_2$ and α-$2H$-$MoTe_2$ were grown by the chemical transport method using bromine as the transport agent. The hydrostatic high pressure was generated by a diamond anvil cell. The flat surface of the diamond generating high pressure was 0.6 mm in diameter. The metal gasket was made with Udimet 700, and had a hole of 200 μm. The pressure was measured from the wavelength shift of the R_1 luminescence line of ruby.[24] A mixture of methanol and ethanol (4:1) was used as the pressure transmitting liquid. This mixture becomes solid above about 100 kbar. In order to prevent pressure inhomogeneity, a small sample of $50\times50\times5$ μm^3 and small ruby chips of 10 μm in diameter were used. The Raman scattering experiment was executed in a back-scattering configuration at room temperature. A 100-mW 5145-Å Ar-ion laser, a double monochromator Spex 1400 with holographic gratings and a computer-controlled photon-counting system were used. The cleaved surfaces of MoX_2 were used, and therefore the A_{1g} and E_{2g} modes are observable in this experimental configuration.

Figures 2(a), 2(b), and 2(c) show the pressure dependence of the phonon energies of the A_{1g} and E_{2g} modes in $2H$-MoS_2, $2H$-$MoSe_2$, and α-$2H$-$MoTe_2$, respectively. The lowest energy modes E^2_{2g} are the rigid-layer modes. These energies increase rapidly with an increase of pressure, but the speed of the increase becomes slow above 50 kbar. The phonon energies at atmospheric pressure and the pressure derivatives near atmospheric pressure are listed in Table I with the values of other authors.

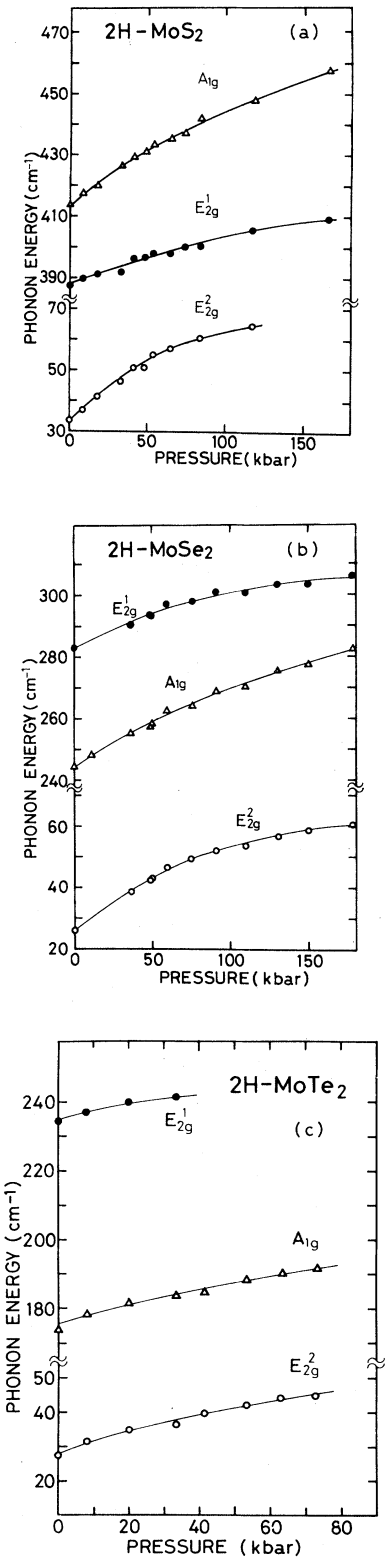

FIG. 2. Pressure-dependent phonon energies of the A_{1g} and E_{2g} modes in $2H$-MoS_2 (a), $2H$-$MoSe_2$ (b), and α-$2H$-$MoTe_2$ (c).

TABLE I. Lattice constants, compressibilities, phonon energies and their pressure derivatives, and interlayer and intralayer shear force constants and their pressure derivatives in $2H$-MoX_2.

		Units	$2H$-MoS_2	$2H$-$MoSe_2$	α-$2H$-$MoTe_2$
Lattice constant[a]	a	Å	3.160	3.288	3.517
	c	Å	2×6.147	2×6.460	2×6.981
	$c/2a$		1.945	1.962	1.984
Intralayer height[a]	$X-M$	Å	3.19	3.23	3.63
		Å	2.41	2.49 ?	2.73
van der Waals gap height[a]		Å	2.96	3.22	3.35
	$X-X$	Å	3.47	3.75	3.92
$2\times$ van der Waals radius of X		Å	3.70	4.00	4.40
Initial compressibility[b]	K_a	$kbar^{-1}$	3.4×10^{-4}		
	K_c		16.4×10^{-4}		
	K		23.2×10^{-4}		
Phonon energy	$\omega(a_{1g})$	cm^{-1}	413	244	174
			409[c]	243.1[d]	171.4[d]
	$\omega(A_{2u})$		470[c]	350[e]	
	$\omega(E_{1g})$		287[c]	168.8[d]	116.8[d]
	$\omega(E_{1u})$		384[c]	286.0[d]	234.5[d]
	$\omega(E^1_{2g})$		387	283	234
			383[c]	283[d]	232.4[d]
	$\omega(E^2_{2g})$		33.5	26	27.5
			33.7[f]	26.9[d]	25.4[d]
	$\partial\omega(A_{1g})/\partial P$	$cm^{-1}\,kbar^{-1}$	0.40	0.31	0.26
			0.37[g]		
	$\partial\omega(E^1_{2g})/\partial P$		0.19	0.23	0.26
			0.18[g]		
	$\partial\omega(E^2_{2g})/\partial P$		0.45	0.36	0.37
Grüneisen constant	$\gamma(A_{1g})$		0.42		
	$\gamma(E^1_{2g})$		0.21		
	$\gamma(E^2_{2g})$		5.8		
Force constant	C^s_b	$dyne\,cm^{-1}$	2.7×10^3	2.6×10^3	3.9×10^3
	$\partial C^s_b/\partial P$	$dyne\,cm^{-1}\,kbar^{-1}$	70	80	110
	C^s_w	$dyne\,cm^{-1}$	1.7×10^5	1.4×10^5	1.1×10^5
	$\partial C^s_w/\partial P$	$dyne\,cm^{-1}\,kbar^{-1}$	110	210	230
	C^s_b/C^s_w		1.6×10^{-2}	1.8×10^{-2}	3.5×10^{-2}
	$\partial(C^s_b/C^s_w)/P$	$kbar^{-1}$	4×10^{-4}	5×10^{-4}	9×10^{-4}

[a]Reference 1. [d]Reference 14. [f]Reference 9.
[b]Reference 23. [e]Reference 16. [g]Reference 19.
[c]Reference 8.

The energies at atmospheric pressure are in good agreement with the data of Wieting *et al.*,[14] and the pressure derivative of the A_{1g} and E^1_{2g} modes in $2H$-MoS_2 are in good agreement with the data of Bagnall *et al.*[19] with the use of the data of Webb *et al.*[23] for the compressibility in $2H$-MoS_2, the mode-Grüneisen constant was calculated as 5.8 for the rigid-layer E^2_{2g} mode. This value is much

larger than the value 0.42 for the A_{1g} mode and 0.21 for the E^1_{2g} mode.

DISCUSSION

Many models have been proposed to calculate the lattice vibration.[9,18,25,26] Wakabayashi[18] showed the necessity of the bond-bending forces and the non-nearest-neighbor interatomic forces coming from the covalent bond between the intralayer atoms, in order to reproduce the phonon dispersion curve observed by his neutron scattering experiment. In this paper a simple linear-chain model proposed by Wieting[26] was adopted. The shear and compressive force constants between the chalcogen planes of the neighboring layers are expressed by C_b^s and C_b^c, respectively. The shear and compressive force constants between the molybdenum and chalcogen planes in a layer are expressed by C_w^s and C_w^c, respectively. The energy of the A_{1g} and E_{2g} modes are

$$\omega^2(A_{1g})=\frac{C_w^c+2C_b^c}{M_x} ,$$

$$\omega^2(E^1_{2g})=\frac{C_w^s}{2M}+\frac{C_b^s}{M_x} + \left[\left(\frac{C_w^s}{2M}+\frac{C_b^s}{M_x}\right)^2-\frac{4C_w^sC_b^s}{M_mM_x}\right]^{1/2} \approx \frac{C_w^s}{M}\left[1+\frac{2M^2}{M_x^2}\left(\frac{C_b^s}{C_w^s}\right)\right] ,$$

$$\omega^2(E^2_{2g})=\frac{C_w^s}{2M}+\frac{C_b^s}{M_x} - \left[\left(\frac{C_w^s}{2M}+\frac{C_b^s}{M_x}\right)^2-\frac{4C_w^sC_b^s}{M_mM_x}\right]^{1/2} \approx \frac{4C_b^s}{M_m+2M_x} ,$$

where M_m and M_x are the atomic masses of molybdenum and chalcogen atoms, and

$$M=M_mM_x/(M_m+2M_x) .$$

The pressure dependences of C_b^s and C_w^s were calculated from the energies of two E_{2g} modes. Figure 3 shows the pressure dependence of C_b^s in MoS_2, $MoSe_2$, and $MoTe_2$. The shear force constant C_b^s rapidly increases with pressure, and doubles around 40 kbar and triples around 80 kbar. The intralayer shear force constant C_w^s decreases from MoS_2 to $MoTe_2$, and the rate of the pressure dependence is small in comparison with C_b^s. Figure 4 shows the ratio between C_b^s and C_w^s. This ratio rapidly increases with pressure, but its value is only 8% even at 150 kbar in 2H-$MoSe_2$. Therefore these materials still have good two-dimensional character at 150 kbar. In these materials, the sulfide is most layerlike. The ratios between C_b^s and C_w^s in molybdenum dichalcogenides are 1 order larger than that in boron nitride, but the rate of pressure dependence in $MoSe_2$ and BN is much the same.[27]

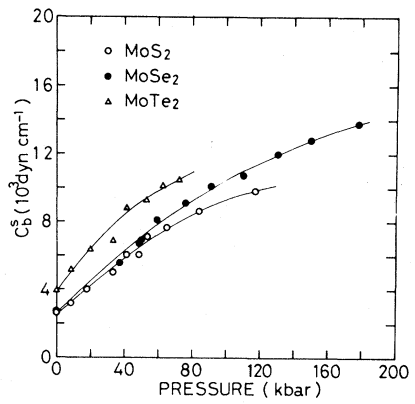

FIG. 3. Pressure dependence of the interlayer shear force constants in MoX_2.

As shown in Table I, the interlayer chalcogen distance is smaller than twice the van der Waals radius of the chalcogen atom. The difference is 0.23 Å in 2H-MoS_2, 0.25 Å in 2H-$MoSe_2$, and 0.48 Å in 2H-$MoTe_2$. The larger difference in 2H-$MoTe_2$ is consistent with the larger interlayer shear force constant C_b^s in $MoTe_2$ as compared with the

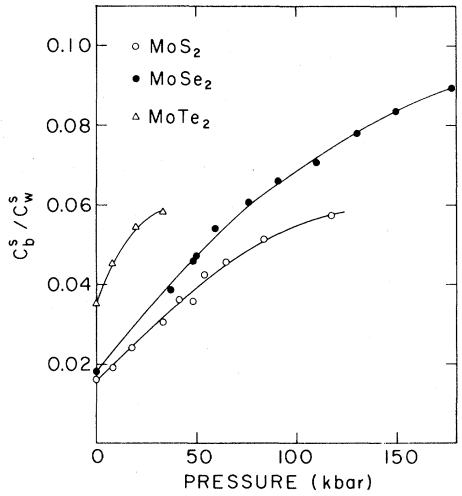

FIG. 4. Pressure dependence of the ratios between the interlayer shear force constants C_b^s and the intralayer shear force constants C_w^s.

other two materials. The large C_b^s and the large transverse effective charge[14] in $MoTe_2$ may relate to the large polarizability of tellurium atoms.

A direct measurement of the van der Waals gap height by x-ray diffraction has not been made under high pressure. The intralayer height increases with pressure by the model of Webb *et al.*,[23] but decreases by the model of Bagnall *et al.*[19] Therefore, we could not obtain the interlayer binding potential as a function of the interlayer distance. No evidence of the phase transition was observed in the experimental pressure range.

ACKNOWLEDGMENTS

We would like to thank K. Murase for discussion, S. Minomura and O. Shimomura for high-pressure technique of the diamond anvil cell, and S. Uchida and S. Tanaka for supplying good crystals of MoS_2 and $MoSe_2$.

[1]J. A. Wilson and A. D. Yoffe, Adv. Phys. 18, 193 (1969).
[2]R. M. White and T. H. Geballe, *Long Range Order in Solids* (Academic, New York, 1979).
[3]J. A. Wilson, F. J. DiSalvo, and S. Mahajan, Adv. Phys. 24, 117 (1975).
[4]R. Clarke, E. Marseglia, and H. P. Hughes, Philos. Mag. B 38, 121 (1978).
[5]C. Manolikas, J. van Landuyt, and S. Amelinckx, Phys. Status Solidi. A 53, 327 (1979).
[6]J. L. Verble and T. J. Wieting, Phys. Rev. Lett. 25, 362 (1970).
[7]R. Zallen and M. Slade, Phys. Rev. B 9, 1627 (1974).
[8]T. J. Wieting and J. L. Verble, Phys. Rev. B 3, 4286 (1970).
[9]J. L. Verble, T. J. Wieting, and P. R. Reed, Solid State Commun. 11, 941 (1972).
[10]O. P. Agnihotri and H. K. Sehgal, Philos. Mag. 26, 753 (1972).
[11]O. P. Agnihotri, H. K. Sehgal, and A. K. Garg, Solid State Commun. 12, 135 (1973).
[12]A. K. Garg, H. K. Sehgal, and O. P. Agnihotri, Solid State Commun. 12, 1261 (1973).
[13]J. M. Chen and C. S. Wang, Solid State Commun. 14, 857 (1974).
[14]T. J. Wieting, A. Grisel, and F. Lévy, Physica 99B, 337 (1980).
[15]T. Sekine, T. Nakashizu, M. Izumi, K. Toyoda, K. Uchinokura, and E. Matsuura, Proceedings of the XV International Conference on the Physics of Semiconductors, Kyoto, 1980 [J. Phys. Soc. Jpn. 49, Suppl. A 551 (1980)].
[16]G. Lucovsky, R. M. White, J. A. Benda, and J. F. Revelli, Phys. Rev. B 7, 3859 (1973).
[17]S. Uchida and S. Tanaka, J. Phys. Soc. Jpn. 45, 153 (1978).
[18]N. Wakabayashi, H. G. Smith, and R. M. Nicklow, Phys. Rev. B 12, 659 (1975).
[19]A. G. Bagnall, W. Y. Liang, E. A. Marseglia, and B. Welber, Physica 99B, 343 (1980).
[20]S. Minomura and H. G. Drickamer, J. Appl. Phys. 34, 3043 (1963).
[21]G. A. N. Connell, J. A. Wilson, and A. D. Yoffe, J. Phys. Chem. Solids 30, 287 (1969).
[22]A. J. Grant, J. A. Wilson, and A. D. Yoffe, Philos. Mag. 25, 625 (1972).
[23]A. W. Webb, J. L. Feldman, E. F. Skelton, L. C. Towle, C. Y. Liu, and I. L. Spain, J. Phys. Chem. Solids 37, 329 (1976).
[24]G. J. Piermarini, S. Block, J. D. Barnett, and R. A. Forman, J. Appl. Phys. 46, 2774 (1975).
[25]R. A. Bromley, Philos. Mag. 23, 1417 (1971).
[26]T. J. Wieting, Solid State Commun. 12, 931 (1973).
[27]T. Kuzuba, Y. Sato, S. Yamaoka, and K. Era, Phys. Rev. B 18, 4440 (1978).